Properties of undoped GaN/InGaN multi-quantum-wells and GaN/InGaN *p-n* junctions prepared by epitaxial lateral overgrowth

A. Y. Polyakov,[1] A. V. Govorkov,[1] N. B. Smirnov,[1] A. V. Markov,[1] In-Hwan Lee,[2] Jin-Woo Ju,[2] S. Yu. Karpov,[3] N. M. Shmidt,[4] and S. J. Pearton[5,a)]
[1]*Institute of Rare Metals, Moscow 119017, B. Tolmachevsky, 5, Russia*
[2]*School of Advanced Materials Engineering and Research Center for Advanced Materials Development, Chonbuk National University, Chonju 561-756, Republic of Korea*
[3]*Softimpact, Ltd., Engels Avenue, 27, S.-Petersburg 194156, Russia*
[4]*Ioffe Physico-Technical Institute, 26 Politechnicheskaya St., St.-Petersburg 194021, Russia*
[5]*Department Materials Science Engineering, University of Florida, Gainesville, Florida 32611, USA*

(Received 26 March 2009; accepted 18 May 2009; published online 23 June 2009)

High resolution x-ray diffraction, electron beam induced current, capacitance-voltage profiling, admittance spectroscopy, deep level transient spectroscopy (DLTS), microcathodoluminescence (MCL) spectra and imaging were performed for multi-quantum-well (MQW) GaN/InGaN *p-n* junctions grown on epitaxial laterally overgrown (ELOG) *n*-GaN platform layers. These experiments show a very good crystalline quality of the MQW ELOG GaN/InGaN structures with a dislocation density of $\sim 10^6$ cm^{-2} in the laterally overgrown ELOG wings regions. Admittance and DLTS spectra show the presence of a prominent electron-trap signal with activation energy ~ 0.4 eV likely originating from electron activation from the lowest occupied state in the quantum wells. MCL spectra clearly show a redshift of luminescence in the laterally grown ELOG wings compared to the normally grown ELOG windows. Modeling based on solving Poisson–Schroedinger equations suggests that the main reason for the observed redshift is a higher indium content in the wings. © *2009 American Institute of Physics*. [DOI: 10.1063/1.3153967]

I. INTRODUCTION

The epitaxial lateral overgrowth (ELOG) technique has been shown to very effectively decrease the dislocation density in GaN films grown on sapphire by metal organic chemical vapor deposition (MOCVD).[1–11] In this method, a GaN template is masked by a dielectric layer with openings, e.g., stripes in a certain direction or circular or shaped holes, followed by GaN film growth on this template. The layer grows vertically in the openings but also laterally over the mask, which results in a much lower dislocation density than in the openings. If the conditions are optimized, a smooth continuous film is obtained in which the low-dislocation density ELOG wing regions are interspersed with high-dislocation-density window regions. This decrease in dislocation density in laterally overgrown regions was proven to have very beneficial effect on performance of GaN-based laser diodes[12] and is expected to improve characteristics of many other devices, such as light emitting diodes (LEDs) or photodetectors. However, one has to remember that ELOG films are characterized by a highly anisotropic growth in the wings and windows regions, by a strong gradient of dislocation density across the structure, and by considerable strain at the boundaries between the high-dislocation-density and low-dislocation-density regions. All this makes it necessary to study in detail electrical properties, deep trap spectra, and luminescent properties of ELOG structures. For GaN ELOG, such studies have been reported previously.[13–18] These experiments showed (i) that the concentration of donor dopants in the laterally overgrown regions is much lower than in the normally grown windows regions, (ii) in capacitance-voltage *C-V* profiling and deep trap spectra measurements the main contribution comes from the laterally overgrown regions and (iii) the density of deep electron and hole traps is considerably lower in the laterally overgrown regions, and decreases with increased layer thickness.[16–18] Much less is known about electrical properties of GaN/InGaN multi-quantum-well (MQW) structures prepared on ELOG GaN. In this paper we present some results of investigations on these structures.

II. EXPERIMENTAL

The GaN/InGaN MQW *p-n* structure was grown as follows. First an undoped *n*-GaN template layer with a thickness of 2.5 μm was deposited on (0001) sapphire by MOCVD. Then a SiO_2 mask pattern with the SiO_2 stripes 12 μm wide going in the [1–100] direction was prepared by photolithography. The stripes were separated by 4 μm gaps. After that, 12 μm of Si doped ELOG GaN was deposited. The doping flow was chosen so that it would give the Si donor concentration of 4×10^{18} cm^{-3} in normally grown MOCVD *n*-GaN. On top of the ELOG GaN we grew five GaN/InGaN MQWs with the GaN barrier thickness designed to be 8 nm and the InGaN QW thickness of 3 nm. The structure was finished with 150 nm of Mg doped *p*-GaN cap layer.

The structures were analyzed by high resolution x-ray diffraction (HRXRD) in the triple axis mode, by microcathodoluminescence (MCL) spectra measurements, and by imaging of the sample surface in monochromatic MCL mode

a)Electronic mail: spear@mse.ufl.edu.

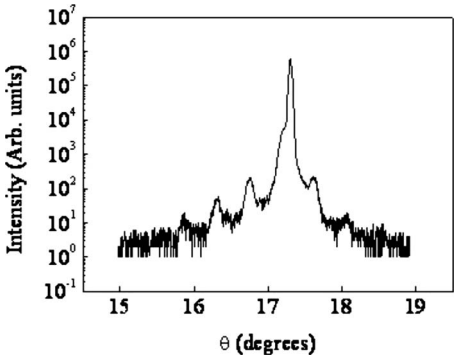

FIG. 1. HRXRD triple axis (0002) reflection pattern for the ELOG GaN/InGaN MQW structure.

and in the electron beam induced current (EBIC) mode. In addition, capacitance-voltage (*C*-V) profiling at various temperatures, admittance spectra,[19] current-voltage (*I-V*) and deep level transient spectroscopy[20] (DLTS) were performed in the temperature range of 85–400 K. For electrical measurements on the GaN/InGaN ELOG MQW *p-n* junctions, 300×400 μm^2 mesa diodes were defined by dry etching in $Cl_2:BCl_3:Ar$. Annealed Ni–Au was used as Ohmic contacts to *p*-type GaN and annealed Ti–Al was used for contacting *n*-type material.[21] More detailed description of the ELOG growth and MQW growth procedures and the experimental setups can be found elsewhere.[15,16,22,23]

III. RESULTS

Figure 1 presents the triple axis HRXRD diffraction pattern for the (0002) reflection of the MQW structure. One can clearly see the zeroth order reflection peak with full width at half maximum =0.1° and well resolved satellite peaks up to fourth order, indicative of excellent crystalline quality. Standard analysis of this diffraction pattern shows that the total thickness of the GaN barrier and the InGaN QW is 10.6 nm, close to designed value. EBIC imaging of the structure showed that the dislocation density in the laterally overgrown ELOG window was $\sim10^6$ cm^{-2} (Fig. 2; dislocations are associated with dark spots in the broad bright ELOG window, the normally grown window region appears as a narrow dark region with a high-dislocation density, measurements with higher magnification showed that the dislocation density in these regions was higher, $\sim10^8$ cm^{-2}).

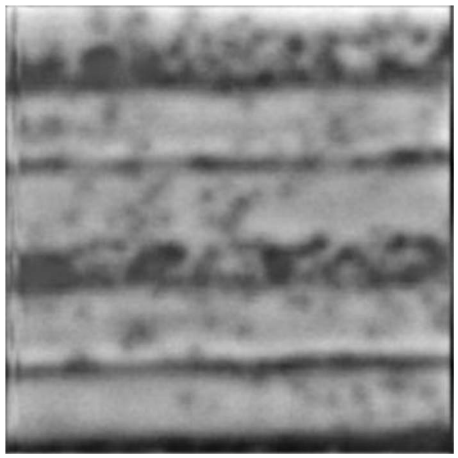

FIG. 2. EBIC image of the studied GaN/InGaN MQW ELOG *p-n* junction; the probing electron beam energy was 25 kV, the beam current was 0.1 nA, the full dimensions of the figure are 30×30 μm^2.

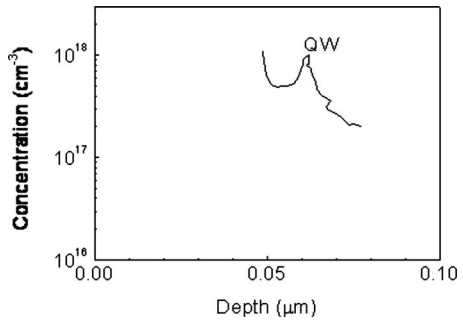

FIG. 3. Room temperature apparent donor concentration profile calculated from *C-V* measurements on the GaN/InGaN MQW ELOG structure

Figure 3 presents the room temperature donor concentration profile obtained from *C-V* measurements. A well defined peak with width close to the period of the MQW structure (11 nm) is present. The data in Fig. 3 suggest that, at 0 V, the space charge region (SCR) boundary is located between the fourth and the fifth QWs and can be swept through the entire MQW region by application of reverse bias of −2 V. Measurements of capacitance dependence on temperature for various frequencies (admittance spectroscopy) showed the presence of two steps at 150–300 and 85–150 K corresponding to activation energies of 0.18 eV with capture cross section of 10^{-13} cm^2 and 0.4 eV with capture cross section of 10^{-9} cm^2, respectively [see actual capacitance characteristics in Fig. 4(a) and the dC/dT derivative in Fig. 4(b); the activation energies were determined as usual from the shift with

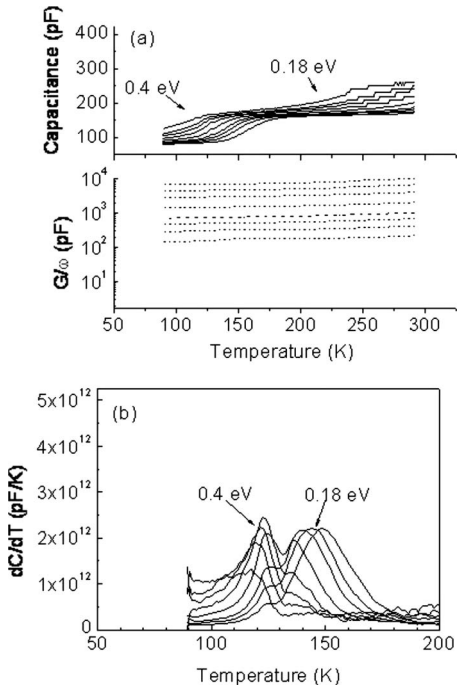

FIG. 4. (a) The temperature dependence of capacitance C and AC conductance divided by frequency G/ω of the studied MQW ELOG structure for frequencies 1, 3, 5, 10, 20, 30, and 50 kHz; (b) the temperature dependence of the dC/dt derivative for the same frequencies.

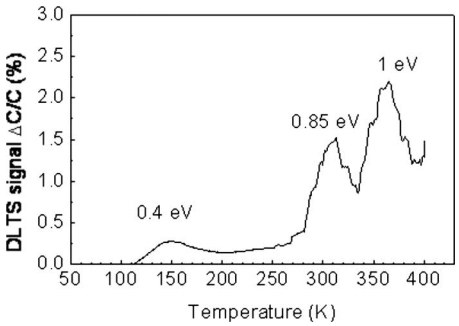

FIG. 5. DLTS spectrum measured on the studied MQW ELOG structure with reverse bias of −1 V, forward bias pulse of 1 V (2 s long) and time windows of 100/1000 ms.

frequency of the center of capacitance steps or the temperatures of the peaks in the derivative spectra;[19] the latter were used instead of the peaks in the ac conductance versus temperature because those were less pronounced due to the problems with leakage current in our diodes, see Fig. 4(a), lower panel].

DLTS spectra measured on our structures showed a low-temperature peak near 150 K with activation energy of 0.4 eV and an abnormally high apparent electron capture cross section of 10^{-9} cm^2 (see Fig. 5). In addition we observed two peaks at 310 and 360 K corresponding to traps with activation energies of 0.86 and 1 eV and electron capture cross section of $\sim 10^{-12}$ cm^2.

MCL spectra were quite different for the laterally overgrown ELOG wing region and the normally grown window regions. Figure 6 compares these spectra for a measurement temperature of 90 K. For the window region, the peak in luminescence is at 2.62 eV (473 nm), whereas for the wing region the luminescence is peaked at 2.69 eV, with a shoulder near 2.62 eV. As a result, the monochromatic MCL image of the structure taken at the longer wavelength of 475 nm shows the ELOG wing stripes as bright regions and the regions growing in the gaps of the SiO_2 mask, the ELOG windows regions, as dark stripes. For the shorter wavelength of 460 nm the contrast for the wings and windows regions is reversed [see Figs. 7(a) and 7(b)].

IV. DISCUSSION

The results above confirm a good crystalline quality of the laterally overgrown ELOG wings material of our MQW

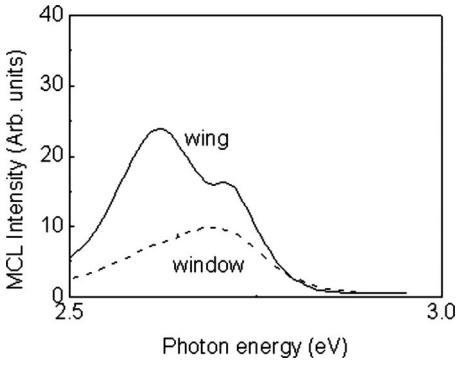

FIG. 6. 90 K MCL spectra taken for the MQW ELOG wing (solid curve) and window (dashed curve) regions.

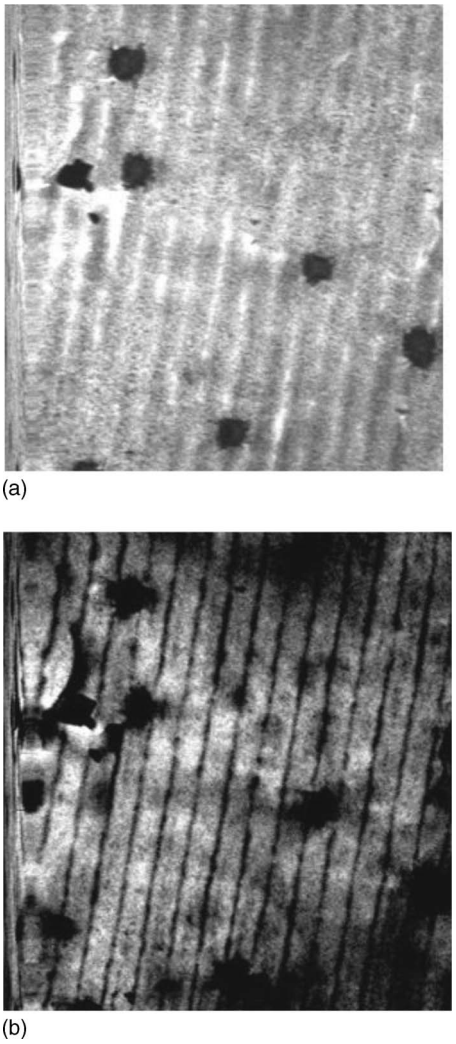

FIG. 7. (a) 90 K MCL image of MQW ELOG structure taken for the 460 nm MCL line; (b) the same for the 475 nm line; the full dimensions of both figures are 100×100 μm^2.

structures and shows a dislocation density of $\sim 10^6$ cm^{-2} from EBIC imaging. HRXRD patterns also point to the low-dislocation density of the ELOG wing material and the good quality of the GaN/InGaN interface. The results of *C-V* profiling show that the SCR boundary at 0 V bias is located between the lowermost and the second lowermost QWs, with the period of the potential profile close to the MQW period designed from previous growth rate calibration and determined from HRXRD data on the actual GaN/InGaN MQW structure. However, the level of donor doping in the ELOG GaN is considerably lower than the one expected from donor doping calibration experiments performed for normally grown MOCVD *n*-GaN films, high 10^{17} cm^{-3} instead of the target 4×10^{18} cm^{-3}. As discussed by us in earlier papers,[17,18] *C-V* measurements on ELOG samples mostly probe the ELOG wing regions where the donor concentration is considerably lower than for the normally grown ELOG windows regions. The reasons for such difference is suspected to be due to the anisotropy of the donors incorporation efficiency for growth in the [0001] direction, the dominant growth direction for the windows region, and the [11–20] direction, the main growth direction in the wings

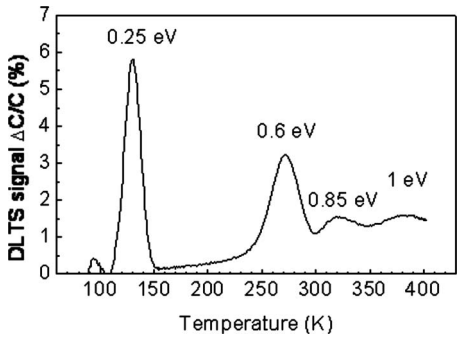

FIG. 8. DLTS spectrum of an undoped ELOG *n*-GaN sample grown similarly to the ELOG GaN portion of our MQW ELOG structures; reverse bias −1 V, forward bias pulse of 1 V (2 s long), time windows of 100/1000 ms.

region.[18] When designing device structures based on GaN/InGaN MQW ELOG, such as LED structures, one has to bear in mind that difference and optimize the doping so as to obtain the desired SCR depth without compromising the leakage current of the structure.

Admittance spectroscopy on the ELOG MQW GaN/InGaN *p-n* junctions shows capacitance freeze-out stages with activation energies of 0.18 and 0.4 eV. The first is due to the freeze out of Mg acceptors that renders the *p*-GaN cap layer equivalent to an insulating film with thickness of 0.15 μm at lowered temperatures. This follows from the good agreement between the activation energy of the process and the known Mg ionization energy.[24] The second process with an abnormally high apparent electron capture cross section is obviously similar to the process responsible for the 0.4 eV peak in DLTS spectra in Fig. 5. Such peaks have been observed in DLTS spectra of good quality GaN/InGaN MQW *p-n* junctions and attributed to electron activation from the lowest filled electron level in the InGaN QW into the GaN barrier.[25] The existence of such a barrier for electrons causes a series resistance specific to the MQW region. This produces a step in capacitance/peak in admittance spectra of our MQW structures.[26] Interestingly, the 0.4 eV electron-trap-like peaks were not detected in DLTS spectra of our GaN/InGaN MQW structures with geometry and indium concentration similar to the present structure, but grown by standard MOCVD.[27] Those MOCVD GaN/InGaN MQWs showed a strong tunneling that dominated *I-V* characteristics and admittance spectra. The lack of the 0.4 eV trap signal in these structures was due to the dominance of the charge relaxation by tunneling in DLTS measurements. The nature of the two other peaks at 0.86 and 1 eV in DLTS spectra in Fig. 5 is not clear. Similar peaks can be observed in the DLTS spectra of undoped ELOG film grown under similar conditions (see Fig. 8), but the high temperature portion of these spectra are dominated by other traps with activation energy 0.6 eV that are absent in DLTS spectra of our GaN/InGaN MQW ELOG structures. We also see that the dominant 0.25 eV electron traps in the undoped ELOG samples are suppressed in the GaN/InGaN MQW ELOG structure.

MCL spectra images show a redshift of the luminescence peak in the ELOG wing regions compared to the ELOG window region. Recently we reported a similar redshift of

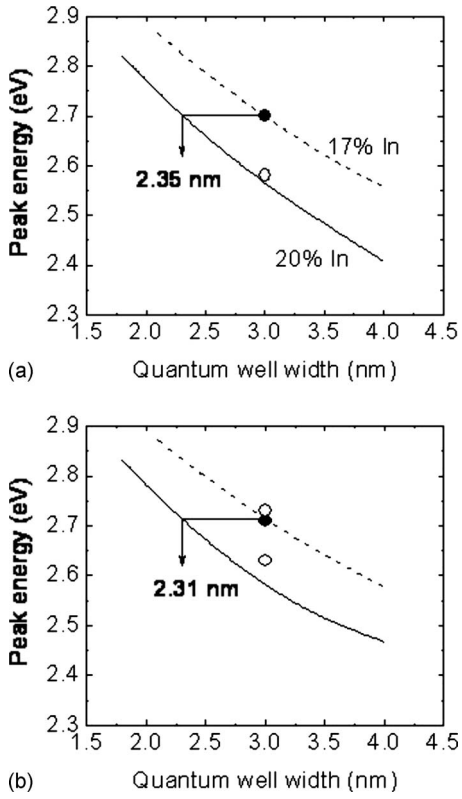

FIG. 9. (a)The results of model calculations of the QW luminescence peak energy for the undoped GaN/InGaN MQW; two In concentrations of 20% (solid curve) and 17% (dashed curve) were tried, experimental MCL peak energy for the MQW ELOG wing region is shown as an open circle, experimental energy for the window region is shown as a solid circle; (b) calculation results for the MQW ELOG *p-n* junction structure, experimental peak, and shoulder energies for the wing region are shown as open circles, the peak energy for the window region is shown as solid circles.

luminescence in undoped GaN/InGaN MQW ELOG structures.[28] The shift was from 2.69 eV in the wing to 2.57 eV in the window, i.e., close to the one observed in Fig. 7. There could be several possible reasons for the observed red shift, the most obvious being an increase in the In concentration in the wing region compared to the window. One has to also to consider the possibility that effective growth rates can be different for growth in different directions. This would suggest that the QWs are thicker in ELOG wings. It is well known that both effects take place for growth on inclined faceted GaN ridges produced by incomplete coalescence of the wing and window regions in ELOG for unoptimized growth conditions, for example, when the lateral growth direction is [1–100]. This phenomenon has been reported in detail and has been proposed as a possible way of getting multicolor emission in GaN MQW LEDs.[29–31] To better understand the dominant mechanism of the red shift in our case we carried out band structure and luminescence modeling using the Poisson–Schroedinger solver SILENSE.[32] Figure 9(a) presents the dependence of the MQW luminescence peak energy as a function of the QW width for the undoped structure. The upper curve corresponds to In concentration of 17%, the lower curve to 20% In (the averaged In concentration calculated from the position of the zero-order diffraction peak in HRXRD pattern in Fig. 1 of Ref. 28 is close to 20%). The open circle corresponds to the mea-

sured peak energy in the window, the closed circle is the measured peak energy in the wing. To achieve the red shift observed in the experiment, the width of the QW should be decreased from 3 nm in the wing to 2.35 nm in the window. Such a large decrease in the QW width is unrealistic. From Fig. 8(a) that the observed shift requires only a 3% increase in the In concentration in the wing compared to the concentration in the window. This increase in concentration is realistic and is in line with the observed In composition change of about 3% occurring when switching the growth direction from [0001] to [11–20].[33] For the *p-n* junction GaN/InGaN MQW ELOG, modeling [Fig. 8(b)] again suggests an unrealistically strong change of the QW thickness in the window (2.31 versus 3 nm in the wing), but only a very moderate change of the In concentration again close to 3%. The MCL peak in the wing of the GaN/InGaN MQW ELOG *p-n* junction structure shows a shoulder with the energy very close to the energy of the MCL peak in the window. The existence of double peaks in GaN/InGaN MQW structures grown by common MOCVD has been reported previously, with a positive correlation between the increase in the In concentration and the existence of strain in the structure.[34] Therefore, the calculations above strongly suggest that the main reason of the red shift observed in the ELOG wing regions of the GaN/InGaN MQWs compared to the window regions is the increase in the In concentration by about 3%. Anisotropy of In incorporation efficiency seems to be a likely reason for such nonuniformity, with the In incorporation efficiency being a function of local strain possibly also playing a role.

V. CONCLUSIONS

GaN/InGaN MQW *p-n* junctions grown by ELOG show improved structural perfection with the dislocation density in the ELOG wing region being $\sim 10^6$ cm^{-2}. Admittance and DLTS spectra show peaks with activation energy of 0.4 eV due to electron activation from the lowest localized level in the QWs into the GaN barriers. Such transitions were not detected in MQW structures with similar geometry prepared by standard MOCVD, because of predominant tunneling in the latter structures. The donor concentration in the ELOG wings of the structure is considerably lower than the value expected from doping experiments on Si doped *n*-GaN films prepared by standard MOCVD. This is in line with earlier reports on lowered Si doping in the wings of ELOG GaN compared to the ELOG windows and is probably due to the anisotropy of Si incorporation. MCL luminescence peaks in the ELOG MQW wings are considerably shifted to the lower energy compared to the window region. Modeling suggests that In concentration increase should be the main factor in this redshift of luminescence. This increase could be a consequence of the In incorporation anisotropy with a role also played by strain.

ACKNOWLEDGMENTS

The work at IRM was supported, in part, by the RFBR Grant Nos. 07-02-13523-ofi-c and 08-02-00058-a. The work at UF is partially supported by the Army Research Office DAAD19-01-1-0603 and DMR 0700416, Dr. L. Hess. The authors thank Dr. E.M. Arakceeva, Dr. I.A. Smirnova, and Dr. M.M. Kulagina at the Ioffe Institute for preparing the diode structures.

[1] H. Sone, S. Nambu, Y. Kawaguchi, M. Yamaguchi, H. Miyake, K. Hiramatsu, Y. Iyechika, T. Maeda, and N. Sawaki, Jpn. J. Appl. Phys., Part 2 **38**, L356 (1999).
[2] C. A. Usui, H. Sunakawa, A. Sakai, and A. A. Yamaguchi, Jpn. J. Appl. Phys., Part 2 **36**, L899 (1997).
[3] A. Kaschner, A. Hoffmann, C. Thomsen, F. Bertram, T. Riemann, J. Christen, K. Hiramatsu, T. Shibata, and N. Sawaki, Appl. Phys. Lett. **74**, 3320 (1999).
[4] J. Holst, A. Kaschner, A. Hoffmann, P. Fischer, F. Bertram, T. Riemann, J. Christen, K. Hiramatsu, T. Shibata, and N. Sawaki, Appl. Phys. Lett. **75**, 3647 (1999).
[5] S. Srinivasan, L. Geng, R. Liu, F. A. Ponce, Y. Narukawa, and S. Tanaka, Appl. Phys. Lett. **83**, 5187 (2003).
[6] H. Wang, C. Chen, Z. Gong, J. Zhang, M. Gaevski, M. Su, J. Yang, and M. Asif Khan, Appl. Phys. Lett. **84**, 499 (2004).
[7] E. Kuokstis, C. Q. Chen, J. W. Yang, M. Shatalov, M. E. Gaevski, V. Adivarahan, and M. Asif Khan, Appl. Phys. Lett. **84**, 2998 (2004).
[8] S. Jursenas, E. Kuokstis, S. Miasojedovas, G. Kurilcik, A. Zukauskas, C. Q. Chen, J. W. Yang, V. Adivarahan, and M. Asif Khan, Appl. Phys. Lett. **85**, 771 (2004).
[9] J. Mei, S. Srinivasan, R. Liu, F. A. Ponce, Y. Narukawa, and T. Mukai, Appl. Phys. Lett. **88**, 141912 (2006).
[10] D. S. Wuu, W. K. Wang, K. S. Wen, S. C. Huang, S. H. Lin, S. Y. Huang, C. F. Lin, and R. H. Horng, Appl. Phys. Lett. **89**, 161105 (2006).
[11] J.-J. Huang, K.-C. Shen, W.-Y. Shiao, Y.-S. Chen, T.-C. Liu, T.-Y. Tang, C.-F. Huang, and C. C. Yang, Appl. Phys. Lett. **92**, 231902 (2008).
[12] S. Nakamura, in *GaN and Related Materials II*, edited by S. J. Pearton (Gordon and Breach Science, the Netherlands, 2000), pp. 1–46.
[13] F. D. Auret, W. E. Meyer, L. Wu, M. Hayes, M. J. Legodi, B. Beaumont, and P. Gibart, Phys. Status Solidi A **201**, 2271 (2004).
[14] I.-H. Lee, A. Y. Polyakov, N. B. Smirnov, A. V. Govorkov, A. V. Markov, and S. J. Pearton, Phys. Status Solidi C **3**, 2087 (2006).
[15] I.-H. Lee, A. Y. Polyakov, N. B. Smirnov, A. V. Govorkov, A. V. Markov, and S. J. Pearton, Thin Solid Films **516**, 2035 (2008).
[16] A. Y. Polyakov, N. B. Smirnov, A. V. Govorkov, A. V. Markov, E. B. Yakimov, P. S. Vergeles, I.-H. Lee, C. R. Lee, and S. J. Pearton, J. Vac. Sci. Technol. B **26**, 990 (2008).
[17] E. B. Yakimov, P. S. Vergeles, A. Y. Polyakov, N. B. Smirnov, A. V. Govorkov I.-H. Lee, C. R. Lee, and S. J. Pearton, Appl. Phys. Lett. **90**, 152114 (2007).
[18] E.B. Yakimov, P.S. Vergeles, A.Y. Polyakov, N.B. Smirnov, A.V. Govorkov, I.-H. Lee, C. R. Lee, and S. J. Pearton, Appl. Phys. Lett. **92**(4), 042118 (2008).
[19] D. L. Losee, J. Appl. Phys. **46**, 2204 (1975).
[20] G. M. Martin, A. Mitonneau, D. Pons, A. Mircea, and D. W. Woodard, J. Phys. C **13**, 3855 (1980).
[21] D. A. Zakgeim, I. P. Smirnova, E. M. Arakceeva, M. M. Kulagina, S. A. Gurevich, V. W. Lundin, A. F. Fomin, A. L. Zakgeim, E. D. Vasil'eva, and G. V. Itkinson, Abstracts of the Fift International Symposium on Blue Laser and Light Emitting Diodes: ISBLLED-2004 (Gyeongju, Korea,2004), pp. 34–35.
[22] A. Y. Polyakov, N. B. Smirnov, A. V. Govorkov, M. Shin, M. Skowronski, and D. W. Greve, J. Appl. Phys. **84**, 870 (1998).
[23] A. Y. Polyakov, N. B. Smirnov, A. V. Govorkov, M. G. Mil'vidskii, A. S. Usikov, B. V. Pushnyi, and W. V. Lundin, Solid-State Electron. **43**, 1929 (1999).
[24] M. Imura, N. Kato, O. Okada, K. Balakrishnan, M. Iwaya, S. Kamiyama, H. Amano, I. Akasaki, T. Noro, T. Takagi, and A. Bandoh, Phys. Status Solidi C **4**, 2502 (2007).
[25] D. V. Davydov, A. L. Zakgeim, F. M. Snegov, M. M. Sobolev, A. E. Chernyakov, A. S. Usikov, and N. M. Shmidt, JETP Lett. **33**, 11 (2007) (in Russian).
[26] D. V. Lang, M. B. Panish, F. Capasso, J. Alam, R. A. Hamm, A. M. Sergent, and W. T. Tsang, Appl. Phys. Lett. **50**, 736 (1987).
[27] A. Y. Polyakov, N. B. Smirnov, A. V. Govorkov, I.-H. Lee, J. Hyeob Baek, N. G. Kolin, V. M. Boiko, and D. I. Merkurisov, and S. J. Pearton, J. Electrochem. Soc. **155**, H31 (2008).
[28] A.Y. Polyakov, N.B. Smirnov, A.V. Govorkov, I.-H. Lee, J.-W. Ju, and S.J. Pearton, Appl. Phys. Lett. **94**, 142103 (2009).

[29]H. Fang, Z. J. Yang, Y. Wang, T. Dai, L. W. Sang, L. B. Zhao, T. J. Yu, and G. Y. Zhang, J. Appl. Phys. **103**, 014908 (2008).
[30]K. Nishizuka, M. Funato, Y. Kawakami, Sg. Fujita, Y. Narukawa, and T. Mukai, Appl. Phys. Lett. **85**, 3122 (2004).
[31]K. Nishizuka, M. Funato, Y. Kawakami, Y. Narukawa, and T. Mukai, Appl. Phys. Lett. **87**, 231901 (2005).
[32]See: www.str-soft.com/products/SILENSE.
[33]T. Suski, G. Franssen, J. Szezko, A. Khachapuridze, M. Krysko, S. Grzanka, R. Czemecki, G. Tagowski, G. Nowak, P. Mensz, L.H. Dmowski, E. Litwin-Staszevska, R. Piotrzkowski, B. Lucznik, I. Grzegory, P. Perlin, and M. Albrecht, Abstracts of the International Workshop on Nitride Semiconductors, IWN2008, Montreux, Switzerland, 2008 (unpublished).
[34]S. Yu. Karpov, R. A. Talalaev, E. V. Yakovlev, and Yu. N. Makarov, "*GaN and Related Alloys*," MRS Symposia Proceedings No. 639 (2001), pp. G3.18.1–3.18.6.